sciendo

Acta Materialia Transylvanica 3/2. (2020) 103–107.
DOI: magyar: https://doi.org/10.33923/amt-2020-02-10
angol: https://doi.org/10.33924/amt-2020-02-10

ACTA MATERIALIA TRANSYLVANICA

Effect of Heat Treatment on the Microstructure of Duplex Stainless Steel Welds

Ferenc TOLNAI,[1] Balázs VARBAI[2]

Budapest University of Technology and Economics, Faculty of Mechanical Engineering, Department of Materials Science and Engineering, Budapest, Hungary

[1] *ferenctolnai1@gmai.com*

[2] *varbai@eik.bme.hu*

Abstract

Duplex stainless steels (DSS) are gaining in popularity due to their characteristic features, excellent mechanical properties, and corrosion resistance. The microstructure of DSSs consists of ferrite up to 50 %, and the rest is built up from austenite. The ferritic microstructure can cause chromium-nitride precipitation because the nitrogen solubility in the ferrite phase is very low below 700 °C. Our research showed that electrochemical etching is an acceptable process for revealing chromium-nitrides. Additionally, our research points out that chromium-nitride acts as a secondary austenite nucleation site.

Keywords*: heat treatment, duplex stainless steels, austenite, electrochemical etching, nitrogen.*

1. Introduction

Duplex stainless steels provide a high-strength alternative to design engineers within the family of stainless steels. However, the welding of duplex steels requires extreme attention and precise observance of technological variables due to the formation of many possible non-equilibrium transformations [1, 2]. To maintain the appropriate 1:1 austenite (γ):ferrite (δ) phase ratio and alloy content, a usually nickel-over alloyed filler material or nitrogen-containing shielding gas, is recommended for the welding of duplex steels [3–4].

Duplex steels are also alloyed with nitrogen (N) because N is an austenite-forming element, which is more soluble in austenite than in ferrite [5]. Therefore, when the delta-ferrite cools from 1100 °C, it becomes supersaturated in nitrogen, resulting in chromium nitride precipitations (Cr_2N). Chemical composition, cooling rate, and ferrite grain size are factors that determine which precipitates appear. Nitrogen-containing shielding gas also plays a significant role in the formation of the austenite phase, so less nitrogen remains in the ferrite phase, and, as a result, less Cr_2N is formed. Secondary austenite (γ_2) is rapidly formed by various temperature-dependent mechanisms [6]. At temperatures between 600 and 800 °C, where diffusion is faster, Widmannstätten-type austenitic phases are formed [6]. Although the N content of the γ_2 phase is higher than that of ferrite, its Cr and Ni contents remain substantially below that of austenite formed from ferrite [6]. In the temperature range of 700–900 °C, another variant of γ_2 appears at the δ/γ phase boundary, which is lower in terms of Cr content [6]. In the present study, we investigated the formation of chromium nitride and secondary austenite phases in the case of TIG welding without filler metal and during post-weld heat treatment.

2. Materials and methods

2.1. Base materials

The base material used for both tungsten inert gas welding (TIG welding) and heat treatment was a conventional X2CrNiMoN22-5-3 (1.4462) duplex steel in the form of a 6 mm thick plate. The chemical composition given by the manufacturer is shown in Table 1.

Table1. *Chemical composition of 1.4462 steel according to the manufacturer's data sheet (%).*

Cr	Ni	Mn	Mo	N	C
22,21	5,76	1,36	3,14	0,164	0,02
Si	**Cu**	**S**	**P**	**Fe**	
0,38	0,30	0,001	0,027	bal.	

2.2. TIG welding and heat treatment

Single-pass butt joints were welded by TIG welding on 200×50×6 mm specimens in the PA (horizontal) position with a welding machine without filler material. Three types of arc energy were used: 0.25 kJ/mm, 0.84 kJ/mm, and 1.57 kJ/mm. These arc energies are in the recommended range of 0.5–2.5 kJ/mm for arc welding of duplex steels [7]. The arc energy was calculated similarly to the heat input, but the thermal efficiency was 1.0. Pure argon (Ar) or 6 % nitrogen shielding gas mixtures (Ar + $6N_2$) were used as shielding gas. The tungsten electrode used in the welding process was 2 % thoriated, 3.2 mm in diameter, with a tip angle of 40°. The automatic welding machine kept the arc length constant at 2 mm in all cases. The shielding gas flow rate was 10 L/min in all cases. The heat treatment was performed in molten salt (50 % NaCl + 50 % KCl) at 800 °C for 10 minutes. The heat treatment was performed only on joints welded with argon shielding gas. The reason for the choice of heat treatment temperature and duration was to observe the formation of the γ_2 phase in the ferritic phase structure.

2.3. Evaluation methods

2.3.1. Microstructure examination

Samples for metallographic analysis were cut with a diamond disk from the welded seam under constant cooling. After cutting, the samples were grinded on 4000 grit sandpaper and then polished with a 3 µm diamond suspension. Metallographic [8] or magnetic [9] examinations can be used to detect austenite and ferrite phases. To calculate the austenite and ferrite phases, Beraha's 2 etchant (85 mL H_2O + 15 mL HCl + 1 g $K_2S_2O_5$) was used, which is suitable for color etching. In images of etched samples, ferrite appears dark, and austenite remains light. To detect possible Cr_2N precipitates, electrochemical etching was performed according to the ISO 17781: 2017 standard. The welded samples were etched in 15 % oxalic acid at 10 V for 10 seconds; this etching method being suitable for the detection of nitride precipitates according to the standard. Oxalic acid etching has previously been successfully used by other researchers to detect carbide and nitride precipitates in ferrite [10, 11], so we also used this electrochemical etching method. The examination of the microstructure was performed with an Olympus PMG-3 optical microscope. Measurement of ferrite content was performed on microstructure images of etched samples taken with an optical microscope, using image analysis software and an area-based method.

3. Results and conclusions

3.1. Microstructure after electrochemical etching

Figure 1 shows a microstructure image after oxalic acid electrochemical etching of the heat-affected zone of the sample welded with 0.25 kJ/mm arc energy and argon shielding gas. It can be seen that oxalic acid electrochemical etching is indeed suitable for the detection of precipitates within the ferrite grain, which are probably chromium nitrides.

The microstructure seen in the images following oxalic acid electrochemical etching shows a similar picture with the results found in the open literature [12–14] These phases have been identified as chromium nitride, so it is likely that in our case, the nitride precipitates were visualized by the applied electrochemical etching. Based on the microstructure analysis following etching, chromium nitride precipitates occurred in the most significant amount in the samples welded with the lowest arc energy, including both shielding

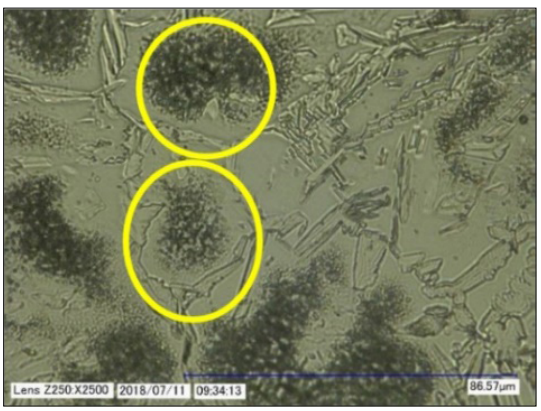

Figure 1. *Possible chromium nitride precipitates inside the ferrite grains in the heat-affected zone. The arc energy was 0.25 kJ/mm, and the shielding gas was argon*

gases used. These nitride precipitates were present inside the ferrite grains and, to a large extent, in the heat-affected zone (Figure 2).

Oxalic acid electrochemical etching, on the other hand, dissolves chromium nitride precipitates, so it was not possible to accurately measure their composition in the present research.

3.2. Microstructure after heat treatment

The heat treatment experiment was performed to achieve the formation of secondary austenite. It can be seen from Figure 3 that the heat treatment applied resulted in an increase in the austenite content in both the weld metal and the heat-affected zone. This is due to the appearance of secondary austenite precipitates in the ferrite particles at the site of the previously observed nitride precipitates. It can also be seen that the formation of secondary austenite started inside the ferrite particles.

Regarding the change in the amount of austenite (Figure 4), it can be observed that the austenite content decreases with increasing arc energy in the case of TIG-welded samples in which pure argon was used as the shielding gas.

The addition of 6 % nitrogen to the shielding gas increased the austenite content of the weld metal because nitrogen is a strong austenite former. In this case, the austenite content of the weld metal is 10% higher than the austenite content of the base materials ~50%.

After the heat treatment of the sample welded with argon shielding gas, the austenite content also increased to 50 %. The increase in the austenite content is the result of the formation of γ_2 in the ferrite grains, in which phase the Cr_2N precipitates that

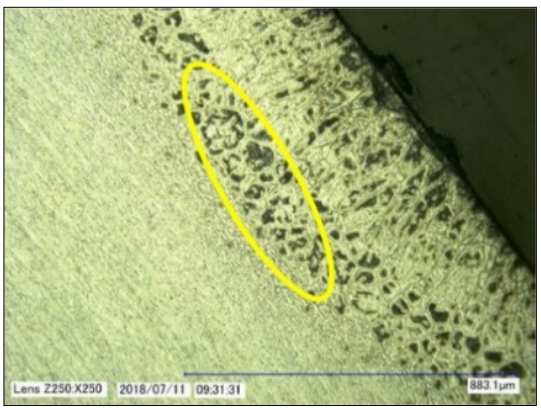

Figure 2. *Possible chromium nitride precipitates inside the ferrite grains in the heat-affected zone. The arc energy was 0.25 kJ/mm, and the shielding gas was argon*

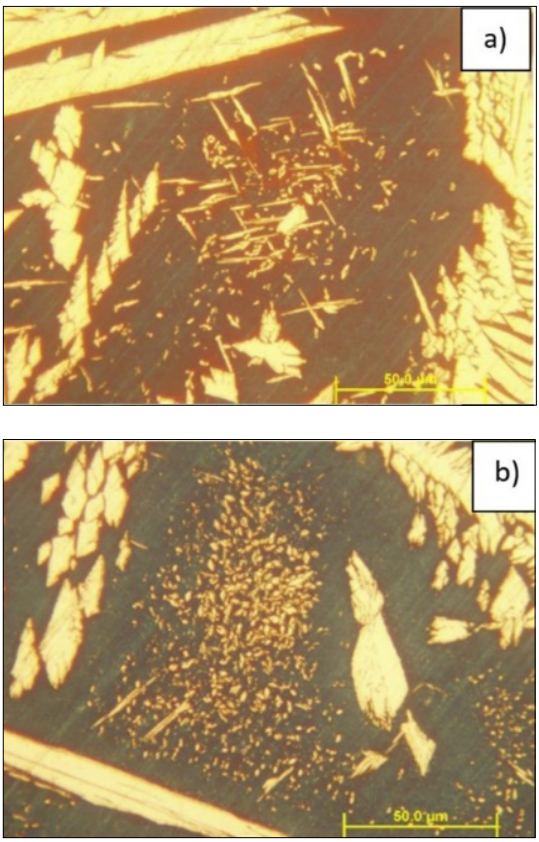

Figure 3. *Microstructure images of the sample welded with argon and the lowest arc energy after heat treatment; (a) weld metal and (b) heat-affected zone*

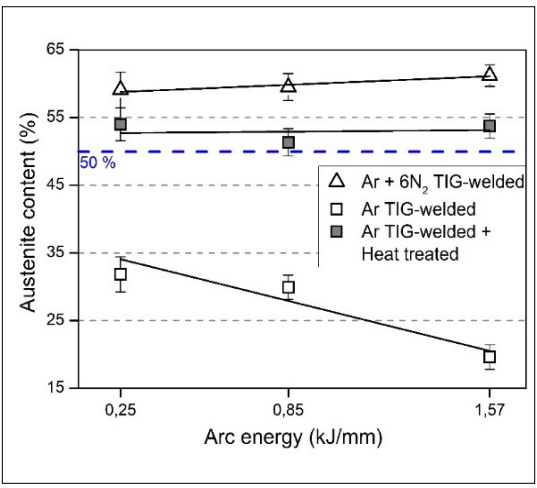

Figure 4. *The austenite content of the weld metal as a function of arc energy, in the case of a sample, welded with both shielding gases and in the case of post-weld heat treatment.*

were present before the heat treatment act as a nucleation site for the formation of the secondary austenite. As the proportion of secondary austenite is high due to heat treatment, we can conclude that γ_2 also plays a very important role in actual, multi-pass welding designs, where it can significantly increase the austenite content of the weld metal during reheating of the previously welded passes [9].

Comparing the results obtained with color etching (Figure 5. a) and electrochemical etching (Figure 5. b), it can be concluded that chromium nitride precipitates led to the formation of secondary austenite in the ferritic heat-affected zone, which is in agreement with the results of other researchers [14].

The formation of secondary austenite in the heat-affected zone and in the weld metal can also occur during the multi-pass welding of duplex steels when the austenite content can be significantly increased [15].

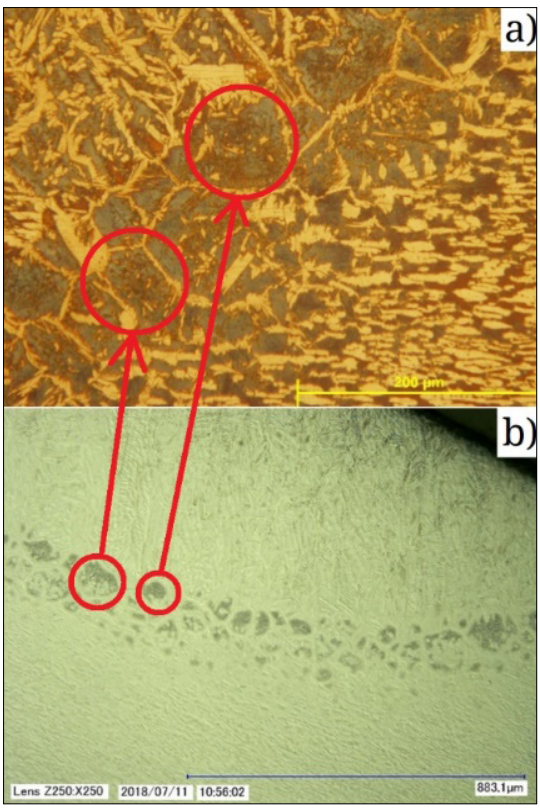

Figure 5. *Microstructure images of the heat-affected zone of the sample welded with argon shielding gas and the lowest arc energy. The relationship between secondary austenite and chromium nitride precipitates is seen in the as-welded image (b) and in the colour etching image after heat treatment (a).*

4. Conclusion

In our research, we performed TIG welding of conventional duplex steel using pure argon and nitrogen-containing shielding gases. Samples welded with pure argon were post-weld heat-treated in molten salt. The applicability of oxalic acid electrochemical etching to the detection of chromium nitride precipitates was also investigated. In addition, we investigated how these precipitates are converted to secondary austenite during heat treatment. Based on our results, it can be stated that oxalic acid electrochemical etching is a suitable method for the detection of chromium nitride precipitates. Chromium nitride precipitates were visible in the heat-affected zone, and after heat treatment, secondary austenite particles formed at the site of the nitride precipitates, which increased the austenite content of the weld metal.

Acknowledgments

The publication of the work reported herein has been supported by the NTP-SZKOLL-19-066 National Talent Programme of the Ministry of Human Capacities. “The research reported in this paper was supported by the BME Nanotechnology and Materials Science TKP2020 IE grant of NKFIH Hungary (BME IE-NAT TKP2020). The research reported in this paper was supported by the BME NC TKP2020 grant of NKFIH Hungary.

References

[1] Uzonyi S., Asztalos L., Dobránszky J.: *Duplex korrózióálló acél durvalemezek hegesztése*. Műszaki Tudományos Közlemények, 3. (2015) 315–318. https://doi.org/10.33895/mtk-2015.03.71

[2] Pálfi N., Berecz T., Fazakas É., Fábián E. R.: *Mikroszerkezeti változások 900 °C-on hőn tartott, majd alakított SAF 2507 típusú duplex korrózióálló acélban.* In OGÉT 2017: XXV. Nemzetközi Gépészeti Konferencia. 25th International Conference on Mechanical Engineering. Cluj, Románia. 2017. 303–306.

[3] Fábián E. R., Dobránszky J., Csizmazia J.: *Duplex acéllemezek lézersugaras hegesztésekor bekövetkező változások*. Műszaki tudományos közlemények, 5. (2016) 141–144. https://doi.org/10.33895/mtk-2016.05

[4] Sándor T.: *Korszerű duplex korrózióálló acélok hegeszthetőségi kérdései.* In: 25. Jubileumi Hegesztési Konferencia. Budapest, Magyarország. 2010. 19–21.

[5] Westin E. M., Johansson M. M., Pettersson R. F. A.: *Effect of nitrogen-containing shielding and backing gas on the pitting corrosion resistance of welded lean duplex stainless steel LDX 2101® (EN*

1.4162, UNS S32101). Welding in the World, 57/4. (2013) 467–476.

[6] Gunn R. N.: *Duplex stainless steels: microstructure, properties and applications*. 1. Ed., Abington Publishing, Abington, 1997. 30–41.

[7] Karlsson L.: *Welding Duplex Stainless Steels – a Review of Current Recommendations*. Welding in the World, 56/05/06. (2012) 1–17.

[8] Lőrinc Zs.: *NAS329J3L duplex acél lézersugaras felületkezelése.* In: Fiatal Műszakiak Tudományos Ülésszaka XIX. Nemzetközi Tudományos Konferencia. Kolozsvár, Románia. 2014. 277–280. https://doi.org/10.36243/fmtu-2014.0 62

[9] Bögre B., Mészáros I.: *Problems of Ferrite Content Determination.* Periodica Polytechica Mechanical Engineering, 64/2. (2020) 150–158. https://doi.org/10.3311/PPme.15022

[10] Nelson D. E., Baeslack W. A., Lippold J. C.: *Characterization of the weld structure in a duplex stainless steel using color metallography.* Metallography, 18/3. (1985) 215–225. https://doi.org/10.1016/0026-0800(85)90043-6

[11] Putz A., Hosseini V. A., Westin E. M., Enzinger N.: *Microstructure investigation of duplex stainless steel welds using arc heat treatment technique.* Welding in the World, 64. (2020) 1135–1147. https://doi.org/10.1007/s40194-020-00906-2

[12] Pettersson N., Pettersson R. F. A., Wessman S.: *Precipitation of Chromium Nitrides in the Super Duplex Stainless Steel 2507.* Metallurgical and Materials Transactions A: Physical Metallurgy and Materials Science, 46/3. (2015) 1062–1072. https://doi.org/10.1007/s11661-014-2718-y

[13] Liao J.: *Nitride precipitation in weld HAZs of a duplex stainless steel.* ISIJ International, 41/5. (2001) 460–467. https://doi.org/10.2355/isijinternational.41.460

[14] Ramirez A. J., Lippold J. C., Brandi S. D.: T*he relationship between chromium nitride and secondary austenite precipitation in duplex stainless steels*. Metallurgical and Materials Transactions A, 34/8. (2003) 1575–1597. https://doi.org/10.1007/s11661-003-0304-9

[15] Pickle T., Henry N., Morriss P., Tennis L., Wagner D., Baumer R. E.: *Root Pass Microstructure in Super Duplex Stainless Steel Multipass Welds.* Welding Journal, 98/5. (2019) 123–134. https://doi.org/ 10.29391/2019.98.010